Analysis of BLEVE overpressure using spherical shock theory

A.M. Birk, R. Eyssette, F. Heymes

Analysis of BLEVE overpressure using spherical shock theory

A.M. Birk [a], R. Eyssette [a,b,*], F. Heymes [b]

[a] Department of Mechanical and Materials Engineering, Queen's University, Canada
[b] LGEI, IMT Mines Ales, Ales, France

A B S T R A C T

The near-field hazards from BLEVE including blast, ground force, drag loading from the rapid liquid phase change and projectiles. There are several correlations available in the literature for the far field blast overpressure from a BLEVE, usually requiring the calculation of the available expansion energy and the application of correction factors. However, there is very little information available for near-field effects and how this is affected by the details of vessel failure.

This work presents near-field blast overpressure data and prediction models to fill in this gap. First, experimental measurements of overpressure in the near-field of a small scale cylindrical controlled BLEVE experiments with propane (V = 0.6 L, d =50 mm, L = 300 mm) were performed. Then, this work establishes a prediction model based solely on the vapour phase properties at failure, using shock tube overpressure prediction and spherical shock propagation models.

The model predicts well the strongest tests and is conservative with all the others. Scaling the model up to larger scale experimental data from literature shows that it is transposable, proposing a simple physics-based prediction model for BLEVE overpressure.

Keywords:
BLEVE
Boiling liquid expanding vapor explosion
Explosion
Overpressure
Experimental results
Blast measurement
Lead shock
Prediction model
Modelling
Spherical shock

1. Background and motivation

It is well known that boiling liquid expanding vapour explosions (BLEVE) produce shock waves and overpressures that can cause significant damage to nearby objects and personnel (Abbasi and Abbasi, 2007). There are several correlations available in the literature for the determination of the far-field blast overpressure from BLEVE. These correlations usually require the calculation of the available energy and the application of correction factors.

It is also important to understand the near-field hazards from BLEVE including blast, ground force, drag loading on local objects from the rapid liquid phase change and projectiles. However, there is very little information available for near-field effects and how this is affected by the details of vessel failure.

One of the key questions about BLEVE blast is its origin. Does it originate from the vapour space or from the flashing liquid? Some existing correlations assume it originates from the liquid and they use the liquid energy to scale the distance (Casal and Salla, 2006). Some recent models such as those by (Van den Berg, 2008) and (Yakush, 2016) assume the blast is from the liquid assuming instantaneous phase change and expansion limited shock buildup.

But there is strong evidence that suggests the liquid flashing is too slow to produce the lead shock. (Baker et al., 1983) stated this many years ago. (Birk et al., 2007) and suggested this in his analysis of the blast measured from 400 L propane tanks. This evidence suggests that the lead shock originates from the vapour and has very little or no contribution from the liquid.

Emergency response personnel need to know the near-field effects from a BLEVE. They also need to now the directional effects from a BLEVE. It is known that the blast in the near-field is different for the vessel top, side and end (Laboureur et al., 2014). There is however very little information available on that matter.

Here we define the near-field as a distance of 5–10 vessel diameters for a horizontal cylindrical vessel. This is the region where the lead shock develops into a full moving shock. (Laboureur et al., 2015) suggested that the shock is formed somewhere around 3–4 vessel diameters from the centre of the vessel.

This paper reports on a small scale series of BLEVE experiments using aluminum tubes (D =50 mm, L = 300 mm) that were weakened to cause failure at specified pressures. These tubes were filled with propane and failed at pressures between 10 and 33 bar. The tubes were filled with liquid propane to fill levels between 10 and

* Corresponding author at: Department of Mechanical and Materials Engineering, Queen's University, Kingston, Ontario, Canada.
E-mail address: eyssette.roland@queensu.ca (R. Eyssette).

90 % of the tube volume. The weakened length along the tubes was between 50 and 150 mm.

The tube failures were recorded using high-speed video and high-speed shadowgraph. Pencil type blast gauges were used to measure overpressures at several distances from the top, sides and ends of the vessel. Load cells were used to record ground loading during the event. The tube also had a window on one end so the boiling wave at the tube end could be recorded.

This paper will focus on a new physics-based method to analyze the peak overpressure from the lead shock produced by a BLEVE. It will also show that the overpressure can be predicted from the vapour space volume and failure pressure.

2. Dimensional analysis

This dimensional analysis is based on the following assumptions:

i) fluid viscosity is not an important factor in this analysis
ii) important fluid properties include the liquid and vapour density, the surface tension, and the ratio of specific heats k (isentropic expansion factor) of the vapour.
iii) the lead shock overpressure is a function of how quickly the vessel opens and the volume and pressure-temperature of the vapour space.
iv) the speed of this vessel opening is determined by the cut length, the tube wall thickness and material and the failure pressure which is determined by the liquid temperature.
v) the ground force depends on how quickly the vessel opens, the failure pressure, the tube size and the liquid fill level
vi) the surface tension is included to acknowledge there may be a scale effect that we are not including with our small scale apparatus. However it should be noted that similar processes and overpressures have been observed in vessels with diameters twenty times (volumes 1800/0.6 = 3000 times) greater than in these experiments (Birk and VanderSteen, 2006).

The dimensional analysis has been conducted and suggests the following functional relationship for the blast overpressure and ground loading.

$$\frac{\Delta P_s}{\Delta P_{st}} = f\left[\frac{L}{D}, \frac{L_c}{L}, \frac{t_w}{D}, \frac{P_f D}{2 t_w \sigma_{yld}}, f, \frac{T}{T_{sl}}, \frac{T}{T_{sat}}, \frac{\sigma d_d}{P_f D^2}, \frac{R}{R_o}, k, \frac{\rho_g}{\rho_f}\right] \quad (1)$$

where,

D = tube diameter
d_d = vapour bubble or liquid droplet diameter
σ = surface tension
σ_{yld} = yield strength of the tube material
L = tube length
L_c = weakened cut length
t_w = tube wall thickness
f = liquid fill volume fraction
T = liquid temperature
T_{sl} = atmospheric superheat limit temperature
T_{sat} = saturation temperature for failure pressure. We assume here that $T_{vap} = T_{liq} = T_{sat}$
P_f = failure pressure
ΔP_{st} = overpressure from 1D shock tube equation from P_f and T and $k = c_p/c_v$
ΔP_s = peak overpressure at R
R_o = radius of sphere with same volume as vapour space

In this series of experiments, a number of these variables and groups were held constant (D, L, t_w, propane, aluminum, k and d_d and $T/T_{sat} = 1$). We have also removed the ratio T/T_{sl} because experience suggests this is not a very important parameter for real world pressure vessels with rough walls and impurities in the liquid. Moreover, thermal stratification was not considered, because there was none in the small-scale experiment. With these the equations simplify to:

$$\frac{\Delta P_s}{\Delta P_{st}} = f\left[\frac{L_c}{L}, f, \frac{R}{R_o}\right] \quad (2)$$

In this paper, we will focus on defining R/R_o, which partially accounts for f.

Fig. 1. Image of opened tube with flattened part still attached to ends. Failure runs along top of tube and then turns circumferentially at the ends of the weakened length.

3. Apparatus

To study these details, we designed and manufactured a small scale apparatus that would allow us to record detailed images of the failure process and to measure overpressures very near to the vessel (within $R/D_{tube} = 0.175/0.050 = 3.5$).

The objective was to have a small scale apparatus with failure modes similar to large scale horizontal cylinders heated (weakened) at the top in the vapour space. In these vessels the failure starts as a pin hole that grows along the top in the axial direction. This crack opening then turns in the circumferential direction at the end of the weakened zone or at the tank ends. This results in the full opening of the vessel and the flattening of the open vessel on the ground. It is very difficult and expensive to do such tests in large scale. For this reason, our apparatus was small.

The apparatus involved an aluminum tube with D =50 mm and L = 300 mm and nominal wall thickness of 1.6 mm. The apparatus and failure was designed to be representative of a cylinder failing and suffering a BLEVE at its top and centre. Figs. 1–4 show the failure of the small tubes compared to the failure of larger pressure vessels. Further details of this apparatus will be given later in the paper.

The apparatus was designed and constructed to study the early moments of a BLEVE in a weakened cylinder. The key design objectives were:

i) make the vessel as large as possible but small enough to be financially feasible to do many tests
ii) the failure mode should be similar to what is seen in practice with horizontal cylindrical pressure vessels
iii) allow for variable L/D and weakened length L_c/D
iv) allow for variable failure pressure P_f
v) allow for variable fill level f.

This apparatus consisted of the following parts:

Fig. 2. image of failed tube with separated part of wall flattened on blast plate. Weakened length is the upper and lower free edges of the flattened part.

Fig. 3. 0.4 m^3 pressure vessel suffering a BLEVE. Failure runs along top of vessel and turns circumferentially at the ends. This vessel eventually flattened on the ground.

Fig. 4. 0.4 m^3 pressure vessel after suffering a BLEVE. Failure runs along top of vessel and turns circumferentially at the ends. Cylinder flattened on the ground.

i) aluminum tube (6061 T6 annealed to T0) with D =50 mm and L = 300 mm with wall thickness 1.6 mm
ii) top of the tube machined to reduce the wall thickness over length Lc to give desired failure pressure in the range 10–35 bar.
iii) Swagelok end caps. One machined to accept fill and vent lines, two thermocouples (type K 1 mm diameter), pressure transducers (TC-Direct 716-072) and a high speed pressure transducer (PCB M101A02). The other end cap machined to have a 30 mm diameter window
iv) electric heater machined to cover bottom 30 % of tube surface
v) cradle to hold tube in position
vi) blast plate below tube supported on high speed load cells (PCB M202B)
vii) pencil type blast gauges (PCB 137A23) at various positions
viii) high speed video viewing window end, tube side and top (high speed cameras available: Phantom V711, V2512, VEO710 and Photron SA3)
ix) High speed shadowgraph viewing side and end (same cameras)
x) electric valves to allow for purging, fill and venting the tube

Fig. 5 shows a schematic of the apparatus. Further details of the apparatus can be found in (Eyssette, 2018)

3.1. Test procedure

The tests were conducted indoors in a large high ceiling, well ventilated lab (Spark facility). The test procedure was as follows:

i) the tube was assembled with the end caps and mounted in the cradle.
ii) all instruments were connected and checked for operation.
iii) the data acquisition systems were turned on and data was recorded.
iv) the tube was purged of air using several fill and vent cycles with propane liquid. Leaks were investigated thanks to a FLIR GF320 infrared camera.
v) the tube was then filled with liquid propane to the desired fill condition.
vi) the electric heater was then turned on to slowly heat the liquid until the tube failed (5–20 minutes heating). Slow heating resulted in tube failure when the von Mises stress (0.866 hoop stress) was near the material yield strength.
vii) the failure process was captured with high speed video and shadowgraph
viii) all data was saved.

In case of emergency propane was vented to a flare.

3.2. Tube failure process

The tubes failed near the top where the tube was weakened by reducing the wall thickness by machining. The failure starts as a pin hole that grows rapidly along the tube axis. At the ends of the weakened length, the failure turns circumferentially, and the tube fully opens as shown in Fig. 1.

As the tube opens the vapour space begins to flow out of the growing opening. Initially it is only the vapour that flows out because the liquid has not been exposed to a pressure reduction. The pressure reduction moves towards the liquid surface at the speed of sound in the vapour. For a 50 % liquid full vessel failing at 20 bar, this takes 125 μs.

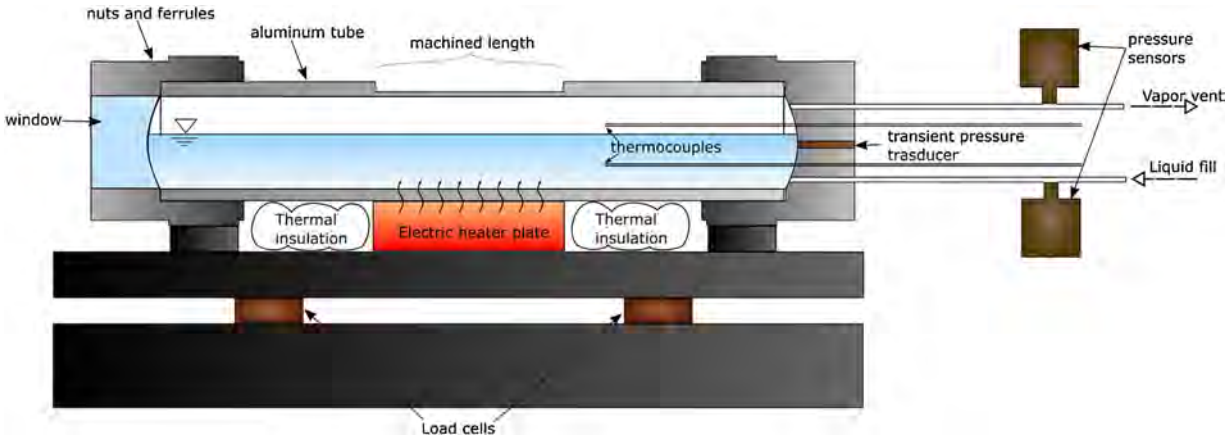

Fig. 5. Schematic diagram of tube apparatus (tube D =50 mm).

The expanding vapour pushes out on the atmosphere and this pushing process creates compression waves. These waves pile up to form a moving shock wave some distance from the tube wall. This is the shock start distance. This shockwave then moves outwards in the surroundings at supersonic speed.

The shock start distance is R_{so} the distance from the tube centerline to the radius where the shock is fully formed. This shock start distance is very important because the shock is not fully formed until this point. Beyond this start position the shock overpressure decays approximately with R_{so}/R where R is the radius from the tube centre.

4. The blast for a BLEVE

The typical far-field blast wave from a BLEVE is shown in Fig. 6. It includes three waves. The lead wave is a supersonic shock followed by an under pressure and this is followed by a second overpressure or weak shock. These two shocks are typical of a spherical gas release. A third wave follows these and it is believed to be from the flashing liquid. It has a more gradual pressure rise and is probably not a shock wave.

A key point to note is that the plot on the left is for an aluminum vessel with D =0.05 m while the one on the right is for a steel vessel with D =0.6 m. The larger vessel has a diameter 12 times larger. The time duration from the first peak to the third peak is around 0.1 s for the large vessel and around 0.009 s or a ratio of around 11. This would suggest the duration of the release event scales with the tank diameter. This would be expected if the crack propagation speeds for the two different scales are similar.

Moreover, (Baum and Parry, 1992) suggest that the minimum velocity of the breach growth is around 0.7 times the speed of sound of the pressurized gas (air in this reference) for it to keep growing in the case of pipe ruptures. In some small-scale BLEVE cases, the order of magnitude is 1.2 times the speed of sound of pressurized propane, approximately 240 m/s. (Makino et al., 2009) quantify crack propagation velocity in steel pipes between 100–400 m/s, depending on the failure pressure and stress condition, type of steel and pipe design. These give a range on the possible crack propagation velocities of the large-scale steel vessels.

The third overpressure wave of the flashing liquid is not as strong as the lead shock but it does carry a lot of power. The flashing liquid produces a very large and long duration ground loading and strong drag force loading on objects in the near field. The flashing liquid can also propel the vessel parts over large distances.

5. Analytical solution

The objective of this work was to develop a physics based solution to the lead shock from a BLEVE. This method would apply to vessels that fail near the vessel top when they are filled with both liquid and vapour. The method would not apply to vessels that are 100 % full of liquid or to vessels that fail below the liquid level. We will show that the lead shock from this type of BLEVE is generated by the vapour in the vapour space at the time of failure.

We have developed this method for the shock overpressure measured directly above the bursting vessel when the vessel fails at its top. This is believed to be where the blast is strongest in the near field. The overpressure in the near-field from the sides and ends can then be correlated to this top blast. We expect the blast in the far-field to be more uniform from the top, sides and ends.

We wanted a method that could be used for the near and far field. This method would be physics based and not a curve fit to data with adjustment factors.

We started with the 1D shock tube equation which gives the theoretical shock speed and overpressure that starts with the instantaneous removal of the barrier between the pressurized fluid and the surrounding ambient pressure air. This is a theoretical overpressure if the shock forms at the interface between the high and low pressure. In reality the shock does not form there but rather it forms at some distance from the wall and we called this the shock start distance R_{so} (Birk et al., 2018).

Then we used the Friedman-Whitham solution (Kornegay, 1965) for a spherical shock propagating into an infinite surroundings to model the decay in the overpressure with distance. The actual shape of the vessel is a short cylinder so in the near-field the overpressure may not decay exactly as a sphere, but in the far-field we would expect the spherical model to be good.

The problem with these analytical solutions is that they do not account for real world effects including:

i) the non-instantaneous opening of the vessel
ii) the shape of the opening
iii) the delayed formation of the leading shock wave
iv) the non-spherical release of the fluid

For these reasons we expect this method to determine the upper limit of the possible lead shock blast from a BLEVE. We expect most real world BLEVEs to fall below this curve. But from time to time real world BLEVEs may achieve this upper limit.

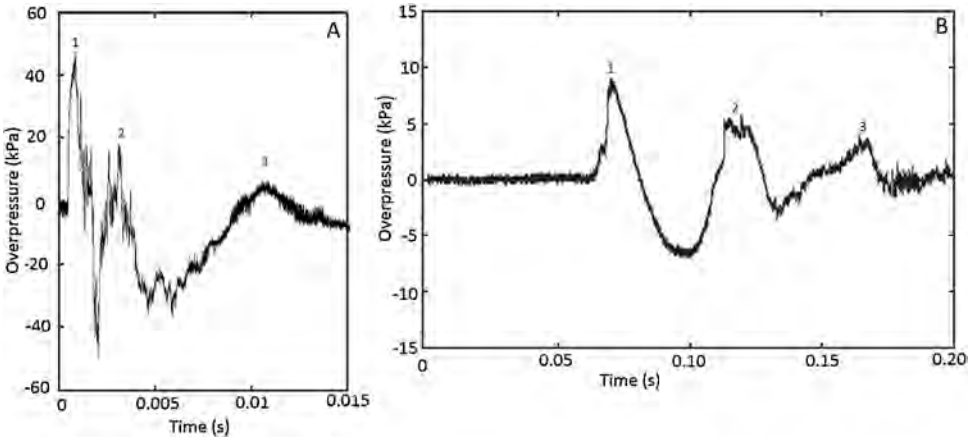

Fig. 6. Typical examples of BLEVE blast waves from propane BLEVEs. On the left is a sample from an aluminum 0.6 L tube BLEVE R = 25.4 mm with L = 300 mm(P_{fail} = 28 bar, $fill_{liq}$ = 63 %, measured 29 cm above the vessel). On the right is a BLEVE of a 2000 l propane tank ((P_{fail} = 18 bar, $fill_{liq}$ = 49 %, measured at 20 m on the side of the vessel) (Birk et al., 2007) 1) lead shock, 2) second overpressure from vapour space release, 3) overpressure (not shock) from liquid flashing.

Fig. 7. Two samples of tubes that failed while filled with both liquid and vapour propane.

The variables in this work included the failure pressure P_f and vapour temperature, the liquid fill fraction f in the vessel and the length of the weakened area L_c in the tube wall where the failure initiates. When the tubes fail, this weakened area opens fully as shown in Fig. 1. Sometimes the tubes do not open fully and the lead shock will not be as strong. Such an opening is shown in Fig. 7. In both cases the failure was at 18 bar with a short cut length. In both cases the tubes only opened on one side. These two tests had almost identical failure conditions. The repeatability of the failure geometry is clearly evident.

The method does not require the calculation of energy. It requires the failure pressure and temperature of the vapour, the ratio of specific heats and the equivalent radius of the spherical release volume which is based on the vapour space volume of the tube.

5.1. Shock tube equation

In a cylindrical shock tube a gas pressurized section with pressure P_4 is separated from a low pressure section at pressure P_1 by a thin partition. When the partition is suddenly removed the high pressure gas expands into the low pressure gas and a 1D normal shock is formed. The one dimensional shock tube equation for an ideal gas is (Baker et al., 1983):

$$\frac{P_4}{P_1}\left[1-\frac{a_1(k_4-1)}{a_4(k_1-1)}(M_o-1/M_o)\right]^{\frac{2k_4}{(k_4-1)}}=\frac{2k_1M_o^2-k_1+1}{k_1+1} \quad (4)$$

Where

P_4 = pressure on the high pressure side of the partition

P_1 = pressure on the low pressure side of the partition

k_1 = ratio of specific heats for the lower pressure gas (air, k_1 = 1.4)

k_4 = ratio of specific heats for the high pressure gas (propane vapour k_4, to define)

M_o = Mach number of shock formed at interface

a_1 = speed of sound in low pressure gas (air) = $(k_1\ R_1\ T_1)^{1/2}$

a_4 = speed of sound in high pressure gas (propane)

In this work we used k_1 = 1.4 for air and k_4 = 1–1.1 for slightly superheated propane vapour.

This gives the Mach number of the moving shock created by the pressure difference when the partition is suddenly removed. From this Mach number it is possible to determine the pressures and temperatures for the moving shock from the normal shock relations.

5.2. Normal shock relations

The static pressures associated with the moving shock are obtained by moving with shock to make it steady so we can use the normal shock relations for a steady 1D normal shock (White, 2008).

$$M_2^2=\frac{(k-1)M_1^2+2}{2kM_1^2-(k-1)} \quad (5)$$

$$\frac{P_2}{P_1}=\frac{1}{k+1}\left[2kM_1^2-(k-1)\right] \quad (6)$$

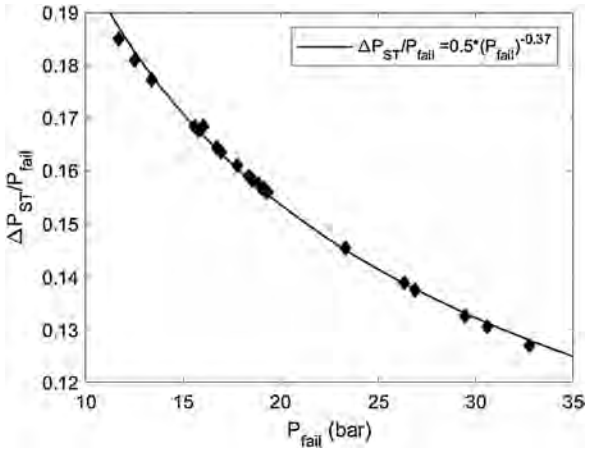

Fig. 8. The shock overpressure from the shock tube equation ΔPst normalized by the failure pressure Pf vs the failure pressure for propane using k = 1.

$$\frac{T_2}{T_1} = \left[2 + (k-1)M_1^2\right] \frac{2kM_1^2 - (k-1)}{(k+1)^2 M_1^2} \tag{7}$$

Where

M_1 = Mach number on the supersonic side of the shock = $V_s/(kRT_1)^{0.5}$

M_2 = Mach number on the subsonic side of the shock = $(V_s - V_b)/(kRT_2)^{0.5}$

k = ratio of specific heats

V_s = moving shock speed

V_b = blast wind speed behind moving shock

T_1 = ambient temperature

T_2 = temperature after shock passes

P_2 = static pressure on supersonic side of the shock

P_1 = static pressure on the subsonic side of the shock (101.325 in this case).

To obtain the stagnation pressures we must return to the stationary reference and determine the stagnation pressure and temperature behind the shock from the static pressure and temperature and the blast wind velocity V_b.

Fig. 8 shows how ΔPst/Pf varies with failure pressure Pf for saturated propane. ΔPst is the overpressure calculated from the shock tube equation. As can be seen the fraction of the failure pressure that appears in the shock overpressure decreases with increasing failure pressure.

The decay of this shock overpressure with distance depends on how the shock expands into the surroundings. In this case, we will approximate this by assuming a spherical expansion.

5.3. Friedman-Whitham shock area relation for spherical shock

These equations (Kornegay, 1965) gives the variation in shock strength as the shock area grows as it expands into the surroundings. In this case we are assuming a spherical expansion of an ideal gas.

$$C = Wexp\left[(2k-2)^{-\frac{1}{2}} sin^{-1}\left[\frac{2Y^2 - (k-1)Z^2}{(k+1)^2 M^2}\right]\right]$$

$$W = \left[\frac{R}{R_o}\right]\left[\frac{(Y-Z)^2}{M}\right]\left[Y(k-1)^{1/2} + Z(2k)^{1/2}\right]\left[\frac{2k}{(k-1)}\right]^{1/2} Y^{2/k}$$

$$\text{With} Y^2 = 2kM^2 - k + 1$$
$$Z^2 = (k-1)M^2 + 2 \tag{8}$$

Where

M = Mach number of the shock at R

R_o = radius of the sphere surface where the shock started

k = ratio of specific heats in the gas where the shock is expanding (k = 1.4 for air).

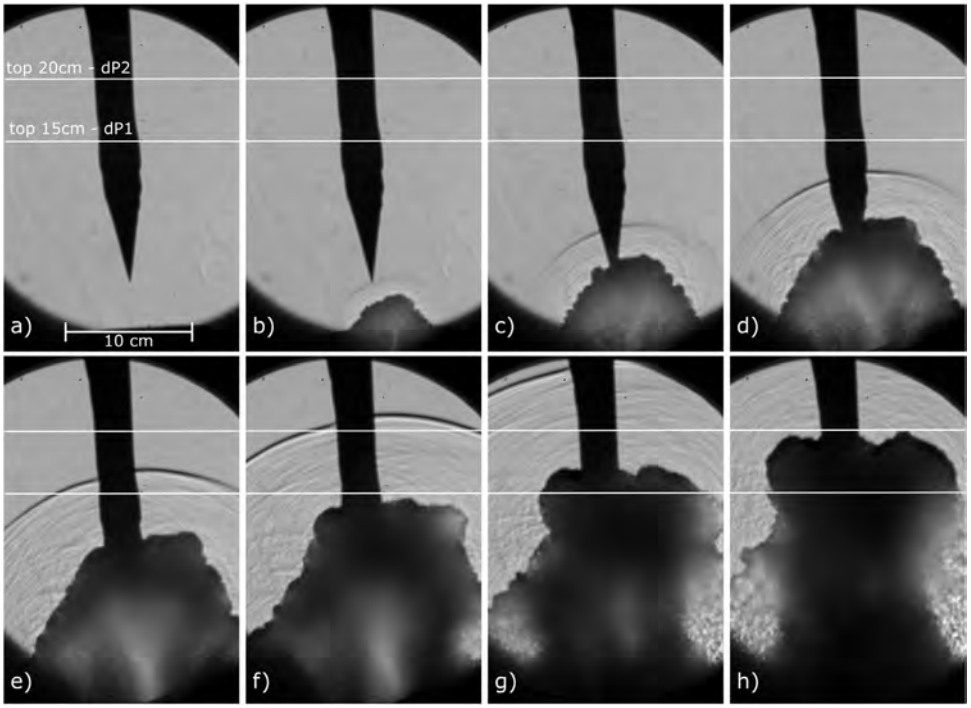

Fig. 9. Sequence of shadow graphs showing formation of lead shock some distance from the tube wall. Shock is formed in frame d and e. Distance to form shock is R_{so}/R_{tube} = 5–6 or R_{so}/D_{tube} =. 2.5–3.

The integration constant C is obtained when $R/R_o = 1$ and $M = M_o$. In this case M_o is obtained from the 1D shock tube relation. R_o is the radius of the sphere of vapour.

5.4. Non spherical release

In this study the R_o is the radius of the spherical release. In this work we did not have a true spherical release. The volume in this case is the vapour space volume along the length of the weakened tube length. If the failure is very rapid, we believe it can be approximated by a spherical release.

In this study we calculated two different radii for the equivalent sphere R_{oc} and R_o. R_{oc} only includes the vapour space volume along the weakened cut length of the tube. R_o includes the entire vapour space. The equations for these are given below:

$$R_{oc} = \left[\frac{3L_c(1-f)V_{tube}}{4\pi L}\right]^{1/3} \tag{9}$$

And

$$R_o = \left[\frac{3(1-f)V_{tube}}{4\pi}\right]^{1/3} \tag{10}$$

Where

V_{tube} = tube volume
L_c = cut length
L = tube length
f = liquid fill fraction

Another issue to consider is whether the vessel failed on the ground or above the ground. If the failure is on the ground, then the release is a hemisphere not a sphere. This requires another starting radius R_{oh}

$$R_{oh} = \left[\frac{3(1-f)V_{tube}}{2\pi}\right]^{1/3} \tag{11}$$

6. Results

The results presented here come in two parts that were slightly different. First we will show the test results from 2017. In these tests the tube was mounted on a pedestal about 1 m above the ground. This was done to simplify the setup of cameras. Then we will look at some results from 2015. These tests were done with tube much closer to the ground.

6.1. Results

The measured maximum overpressures generated by the lead shock are presented here for five sample cases. This shock was measured at the top of the bursting cylinder at 15, 20, 30, 40 and 300 cm from the tube surface (17.5, 22.5, 32.5, 42.5 and 302.5 cm from tube centre) The R/R_o is taken from the tube centre (R_{tube} = 2.54 cm).

As can be seen from Table 1, the highest overpressures were observed with the highest burst pressures, middle fill levels and the longest cut lengths. These were the cases with the fastest tube opening.

An important detail to notice is that in some cases the nearest blast gage (at 15 cm) does not measure the highest overpressure. This suggests the shock has not fully formed by this distance. It is known (Rothkopf and Low, 1976) that the shock does not form immediately at the failure surface. With a non-instantaneous opening, compression waves leave the vessel and pile up to form a shock at some distance away from where the wall was. This shock start distance is given the symbol R_{so}.

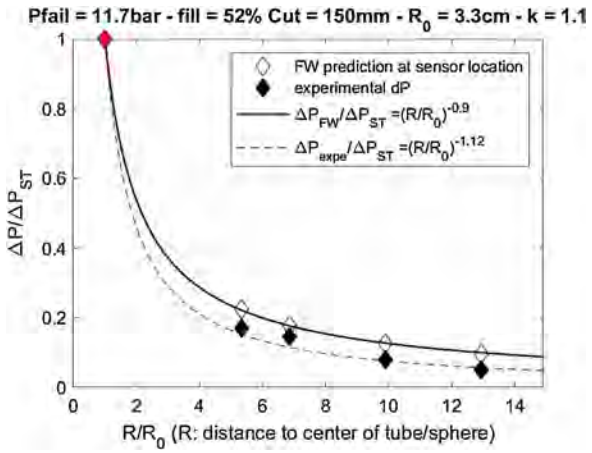

Fig. 10. $\Delta Ps/\Delta Pst$ vs R/R_{oc} for Test 2.

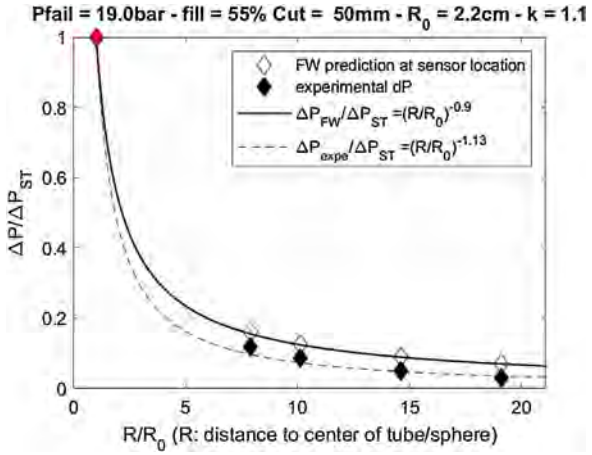

Fig. 11. $\Delta Ps/\Delta Pst$ vs R/R_{oc} for Test 9 (partial opening).

When the shock does fully form it can be related to the theoretical overpressure predicted by the shock tube equation using the formula.

$$\frac{\Delta P_{so}}{\Delta P_{st}} = \left[\frac{R_{so}}{R_o}\right]^n \tag{12}$$

Where

ΔP_{so} = overpressure where shock forms
ΔP_{st} = overpressure predicted from 1D shock tube equation
R_o = radius of equivalent sphere
R_{so} = radius to where shock forms
n = exponent near -1

It is believed the actual overpressure does not start with ΔP_{st} but starts from some lower value and increases in value to ΔP_{so} at the location where the shock is fully formed. From this shock starting position at R_{so} the overpressure ΔPs declines with increasing R/R_o. The shock moves out nearly as a sphere and the growing area gives a decline in overpressure as defined by the F–W solution.

The exact location of R_{so} is difficult to determine even with high speed shadowgraph. Fig. 9 shows a sequence of shadowgraphs. From these images we see a clear shock has formed in frames d) and e) at a R_{so}/R_{tube} of around 5–6 or R_{so} = 13 cm. This is just before the neared blast gage which is located at R = 17.5 cm from the center of the tube.

The following figures (Figs. 10–14) show the data plotted as $\Delta Ps/\Delta Pst$ vs R/R_o where ΔPs is the peak overpressure of the lead shock measured from directly above the tube. The point plotted at $R/R_o = 1$ is the ratio of the overpressure ΔPs divided by ΔPst from

Table 1
Experimental Results (peak overpressure at 15, 20, 30, 40 and 300 cm from tube top).

Test #	P_{fail} (kPa)	T_{fail} Deg C	Fill	Cut (mm)	ΔP 15 cm (kPa)	ΔP 20 cm (kPa)	ΔP 30 cm (kPa)	ΔP 40 cm (kPa)	ΔP 3 m (kPa)
2	1166	33.1	0.52	150	34.6	29.6	16.0	10.1	1.1
9	1901	53.8	0.55	50	32.5	24.0	13.7	8.6	1.0
14	1834	52.1	0.18	150	59.8	61.3	33.1	22.8	2.6
23	3274	81	0.70	150	78.0	77.9	55.1	41.1	4.1
25	2945	75.5	0.18	150	72.5	73.9	50.9	35.4	3.8

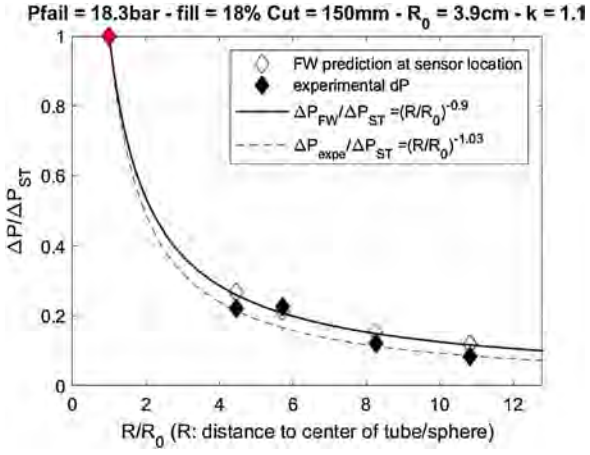

Fig. 12. ΔPs/ΔPst vs R/R_{oc} for Test 14.

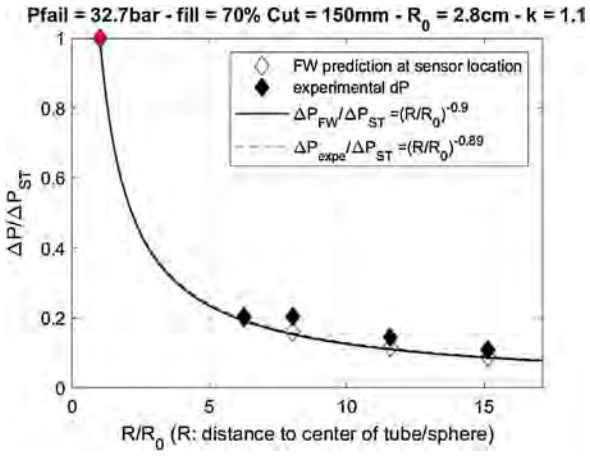

Fig. 13. ΔPs/ΔPst vs R/R_{oc} for Test 23.

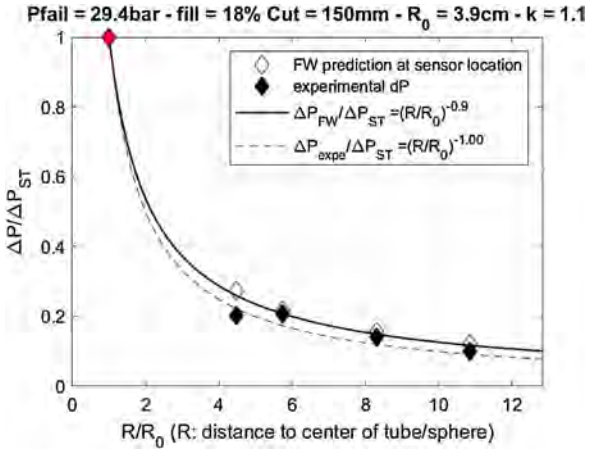

Fig. 14. ΔPs/ΔPst vs R/R_{oc} for Test 25.

the shock tube relation. We have assumed the measured data starts with ΔPs/ΔPst = 1 at r/ro = 1.

For both predicted and measured overpressure data, a power-law curvefit is shown to quantify with simple numbers the trend followed by the data. These will be used as a simple approach to the model at the end of this work because of their easy implementation. But one should remember that the powerlaw are approximations to the model and to the experimental data.

6.2. Observations

When we compare the theory to the peak overpressure results from the small scale tests we see that the results agree very well in one case with the large 150 mm cut, and the highest failure pressure (32,7 bar) and the highest liquid fill of 70 % (i.e. the smallest vapour space). In this case the tube would have failed rapidly and opened fully to release the vapour. The vapour would have been expelled very quickly.

The overpressure decay with distance is correlated well with the following equation. The plots also show power curve fits with the form:

$$\frac{\Delta P_s}{\Delta P_{st}} = \left[\frac{R}{R_o}\right]^n \tag{13}$$

n is a constant and is near -1.

Most of the measured overpressures fall below the F–W theory. The following are reasons for this:

i) the release was non-spherical
ii) the tube opened too slowly
iii) tube did not open fully (full open when opening area = 2 x tube cross sectional area filled with vapour or πD^2 (1-f)/4)

Full opening is when the flow minimum area is 2x the tube cross section filled with vapour (Baum and Butterfield, 1979).

When the tube opens more slowly we see a slower and weaker initial shock, and faster decay of the shock wave with distance relative to the F–W theory.

We can also see the position where the shock achieves full strength. We see this in tests 14, 23 and 25. It appears the over-pressure reaches a maximum somewhere around R/R_o = 6–8.

For the maximum theoretical overpressure, we need a rapid release of the vapour space. The rapid release of the vapour space needs the tube to fully open. High liquid fill levels mean the tube cross sectional area filled with vapour is smaller. This means less opening of the tube is needed to achieve the full open state for the existing vapour volume. Thus the tube will be considered fully open sooner. This will result in a more rapid release of the vapour and a higher initial ΔPs/ΔPst.

The size of the vapour space is very important and it determines the rate of decay of the shock overpressure. In fact it is the Pressure-Volume energy that determines how the shock decays. Our scaled distance here is R/R_o

Note that we have not considered the liquid or vapour energy anywhere in this analysis. We are not assuming expansion limited flashing of the liquid. We are showing the lead shock is due to the

vapour space pressure, temperature and volume alone. Of course the energy in the vapour space is related to these variables.

In most cases the observed pressure in the near-field is below that predicted by the shock tube relation and the F–W method. In only one case (test 23) the measured data is actually above the theory. This suggests that the method can be used for the worst case peak overpressure.

It is believed that most cases fall below the theory because the tubes open more slowly and do not produce the ideal spherical shock.

Another possible explanation for the different decay of the slower release is that the shock is created by a conical release through a partial opening of the wall. The area growth rate of this shock would be more rapid than in the case of a spherical release and for this reason the shock would decay faster. The conical release would transition to a spherical release as the shock moves out. In other words, the angle of the cone would increase until it was a full sphere. The initial shock area would be the outer end surface of the cone. The initial shock speed and overpressure would be the same as predicted from the 1D shock tube equation. But the shock overpressure and Mach number decay would be different because of the different area growth rate with R. This would mean that the shock decays more rapidly because the shock area is increasing for two reasons i) because the cone would spread to become a spherical area, and ii) the sphere area grows with increasing R.

6.3. *Uncertainties*

There are several uncertainties in this analysis including:

i) release is not an ideal gas, it is a superheated or saturated vapour and setting k for propane has some uncertainties.
ii) release is not truly spherical – it is probably somewhere between a spherical and conical release.
iii) In this case we have calculated the effective spherical release radius R_{oc} based on the volume of the vapour space along the cut length. However for long cuts or high liquid fill levels maybe the full cylinder length is more appropriate. To be conservative we will use the full cylinder length.
iv) the creation of the shock is dictated by how the cylinder opens and this will vary from test to test.

The data clearly shows that not all BLEVE produce the theoretical value of the peak overpressure. Most of the time the measured overpressure is below the theoretical. We should be using a conservative method of analysis that gives us the possible overpressure, and not the average. Only in those cases where the vessel opens quickly and fully do we see the theoretical values of the overpressure.

Fig. 15 shows how variations in k_4 affects the calculated start overpressure from the shock tube equation. The decay of the pressure with distance from the F–W theory only depends on the k for air. As can be seen the uncertainty is significant with the start overpressure ranging from about 290–390 kPa (for this case with failure pressure of 29 bar and fill of 18 %).

In this case we wish to be conservative so we will use 1 as the k for propane. If we take the results from Test 23 (the highest burst pressure, highest fill) and adjust as follows:

i) k = 1 instead of 1.1 for propane in shock tube equation
ii) R_o = radius of sphere with volume equal to full vapour space volume (not just along the cut length).

We get the result shown in Fig. 16. As can be seen the agreement is excellent in the near field. In the far-field out to $R/R_o = 86$ the measured ΔPs is 30 % lower than predicted by F–W theory.

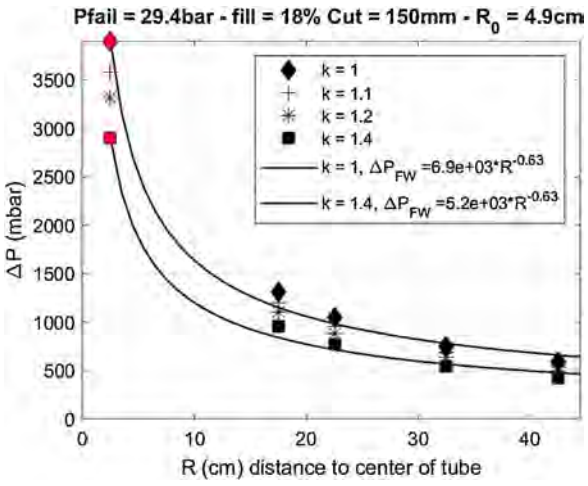

Fig. 15. Variation in Result with k for Propane (test 25).

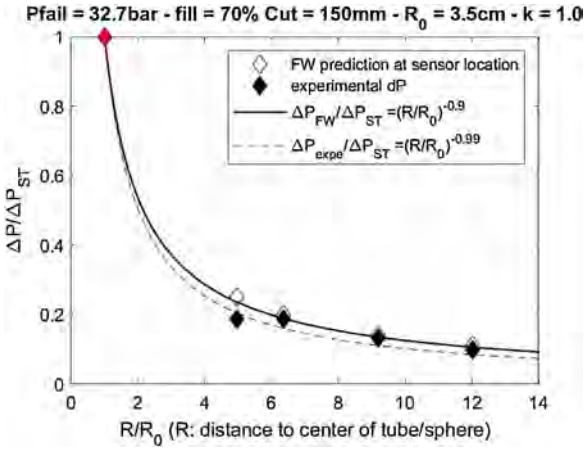

Fig. 16. adjusted result for Test 23, k = 1, R_o = 0.0354 m from full tube length L = 300 mm.

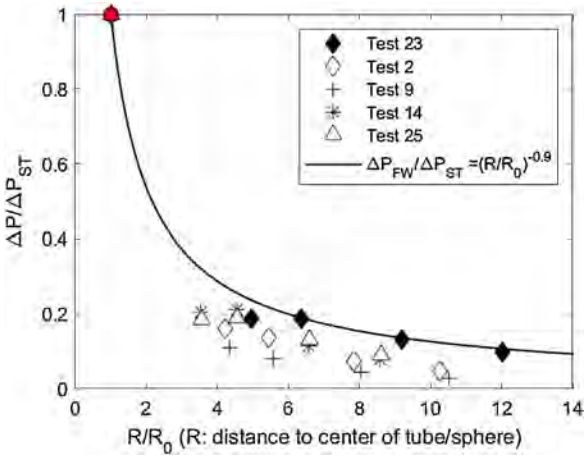

Fig. 17. Peak Overpressure on top from 0.6 L aluminum tube, near and far field, Solid line from FW Theory. All tests.

Figs. 17 and 18 show all the data the five tests presented so far on a single plot. The data is summarized (Table 2). Fig. 17 is a linear scale zoomed on the near-field points while Fig. 18 is semi log to show the points more clearly. Only test 23 agrees well with the theory in the near field. This was the test with the highest failure pressure, medium liquid fill and a long cut. All the other points fall

Table 2
Calculated Results using Shock tube and Friedman-Whitham Method using k = 1.1 for propane, 1.4 for air.

Test #	ΔPst (kPa)	Mo	Ro (m)	ΔP 15 cm (kPa)	ΔP 20 cm (kPa)	ΔP 30 cm (kPa)	ΔP 40 cm (kPa)	ΔP 3 m (kPa)
2	202	1.65	0.033	45.4	35.9	25.4	19.6	3.1
9	276	1.83	0.022	44.3	35.0	24.8	19.2	2.9
14	270	1.81	0.039	72.8	58.0	41.3	32.2	4.7
23	381	2.06	0.028	77.3	61.6	43.9	34.3	5.1
25	358	2.01	0.039	97.9	78.1	56.0	43.7	6.6

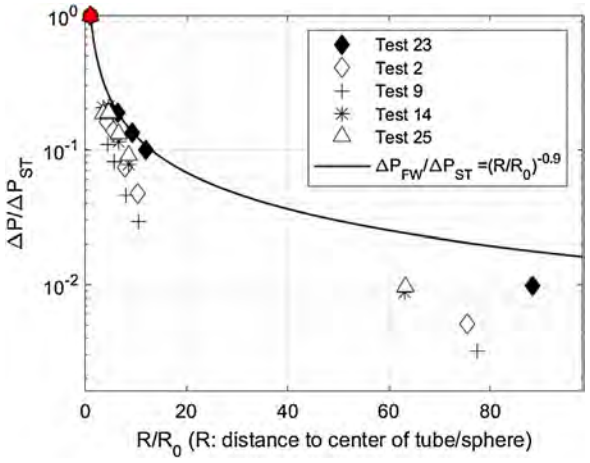

Fig. 18. Peak Overpressure on top from 0.6 L aluminum tube, near and far field, Solid line from FW Theory. All tests with semi-log plot.

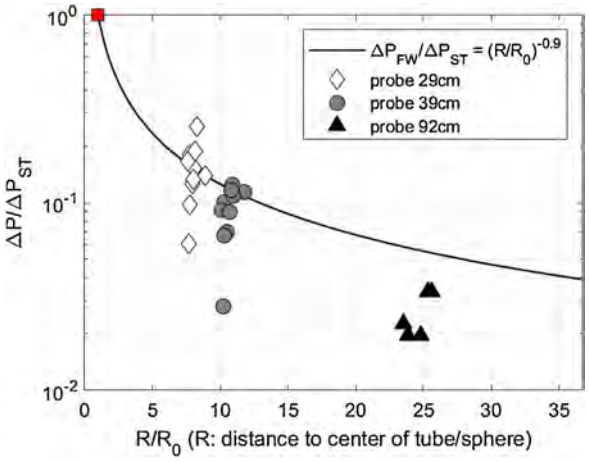

Fig. 19. May 2015 results with Ro based on sphere.

Table 3
Results from May 2015 tests, commercial propane, apparatus on ground.

Test	Pf (bar)	Cut (mm)	Fill (%)	ΔPs (305 mm)	ΔPs (405 mm)	ΔPs (945 mm)
6	40	100	66	65.6	53.5	
7	40	100	66	71.7	58.5	
8	30	100	51	71.5	40.2	
9	28	75	56	47.8	26.6	7.5
10	8	150	50	27.3	15	3.7
11	8	75	48	No BLEVE		
12	37	100	61	113.6	49	15.1
13	31	100	60	76.4	47.1	13.5
14				No burst		
15	29	100	58	51.5	34.5	
16	17	100	53	27	18.5	
17	14	100	52	14.8	6.9	4.8

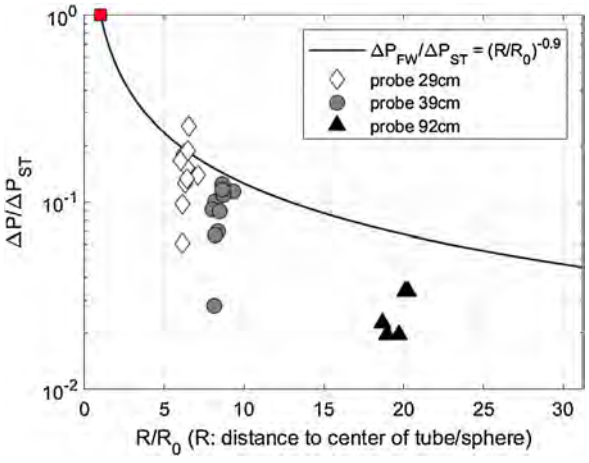

Fig. 20. May 2015 results with Roh based on hemisphere.

below the theory. We believe this is because of the slower opening of the vessel for the other tests. We think this is due to the failure pressure and the cut length. Unfortunately, we need more data with short cut lengths to resolve this detail.

6.4. 2015 results

The results from the May 2015 tests are shown in Table 3. In these tests the tube apparatus was much closer to the ground and the overpressures were measured at different distances from the tube.

The calculated results from the 2015 tests are shown in Fig. 19 and Fig. 20. In the first figure the Ro is based on a spherical release and we see that it does not agree well with the curve for spherical shock. But if we recall these tests were done with the tube near the ground, then this changes the release conditions. If we use the R_{oh} based on the hemisphere, most experimental measurements fall below the prediction curve, except one high overpressure.

This specific test shows a peculiar behavior on the first sensor in comparison with the second and third sensors (Fig. 21). It is possible that there are some additional directional effects in the very near

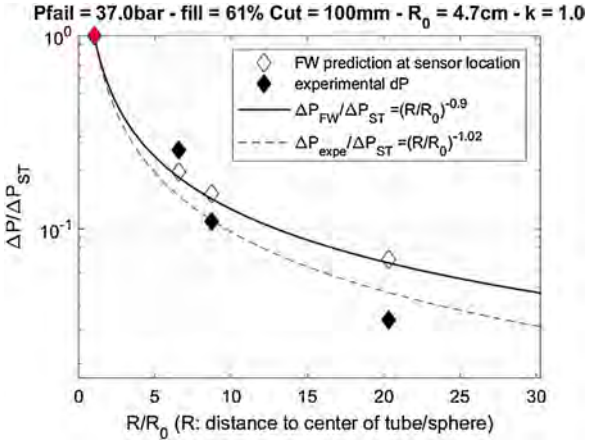

Fig. 21. May 2015, test 12 with Roh based on hemisphere.

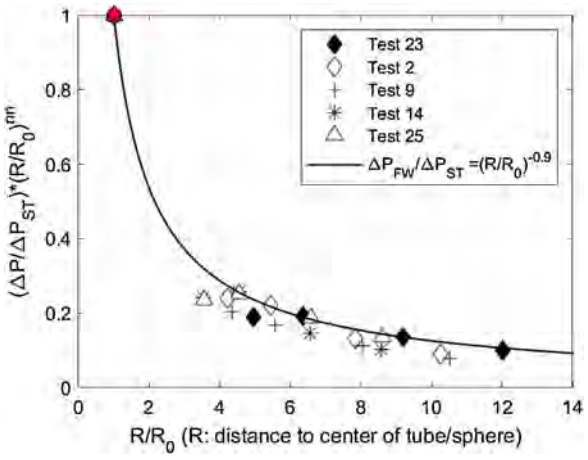

Fig. 22. 2017 results, overpressure data adjusted to fit curve for each test – near field.

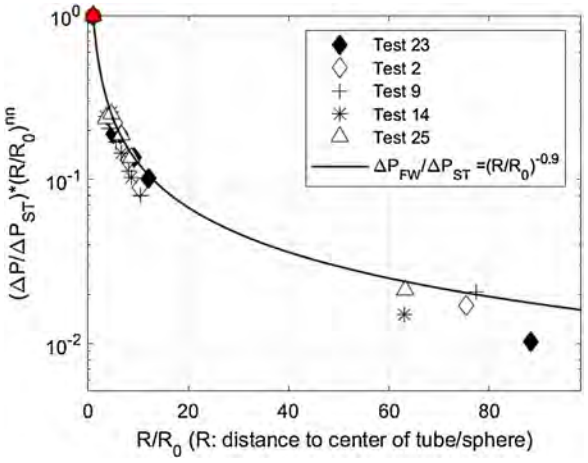

Fig. 23. 2017 results, overpressure data adjusted to fit curve for each test – near and far field.

field. For example, it is possible the blast probe may be sensing both static and some dynamic pressure.

Beside this point, the prediction curves predict well the near-field and overestimate the far-field for all other tests. We saw this in the 2017 results as well.

6.5. *Effect of cut length on BLEVE lead shock overpressure*

If we plot $(\Delta Ps/\Delta Pst)(R/Ro)^{nn}$ vs R/Ro we can shift all the data onto one line if we adjust the exponent nn for each test. By doing this we are basically changing Ro the radius of the sphere of the vapour in the release. In other words, we are changing the fraction of the vapour space included in the release. This is shown in Figs. 22 and 23 for the 2017 results and in Fig. 25 for the 2015 results.

If we then plot nn vs the burst pressure Pf we get Fig. 24. From this Figure we see a decreasing trend for Lc = 150 mm. A few odd points are noted, mostly due to liquid fill level. Since we only have a few data points for other cut lengths, we do not see a trend. But we can see that shorter cut lengths need a higher nn to be well adjusted to the prediction, showing a strong effect of Lc.

Figs. 25 and 26 show the results for the 2015 tests. That data did not adjust to the curve as well as the 2017 results. However the trend for nn with Pf is quite good for the cut length Lc of 100 mm, except for two points that are lower.

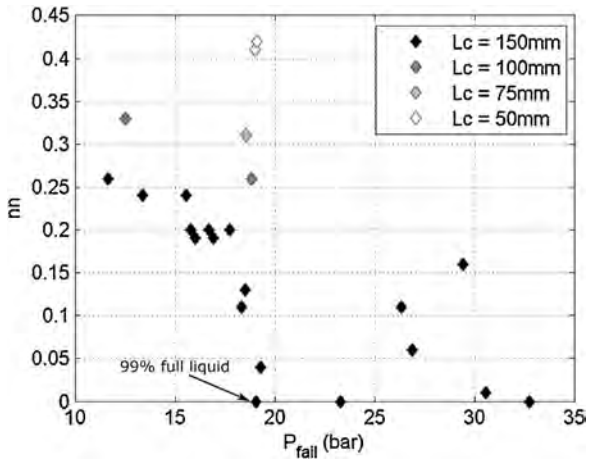

Fig. 24. Exponent nn vs burst pressure for 2017 results.

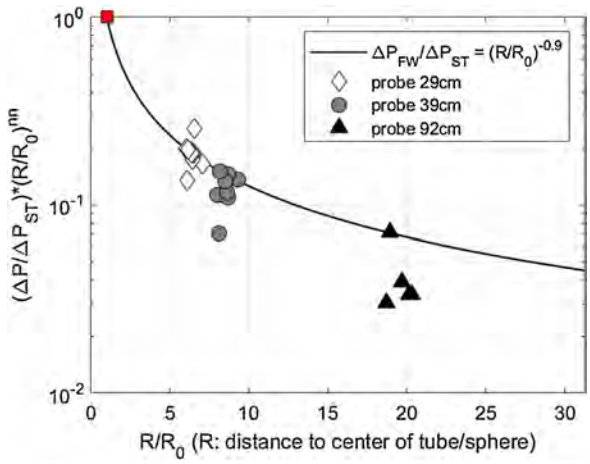

Fig. 25. 2015 Results adjusted with nn for each test to fit the decay curve.

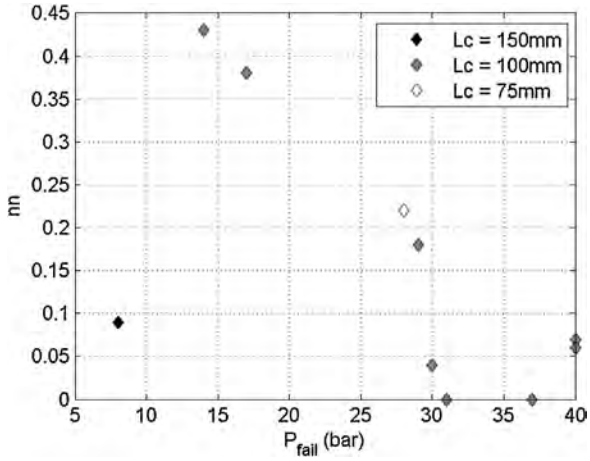

Fig. 26. 2015 Results, exponent nn vs Pf.

We expect the vessel will open faster and more fully with longer Lc and this should give a stronger lead shock and slower decay with R. More tests with short Lc and various fills are needed to confirm this.

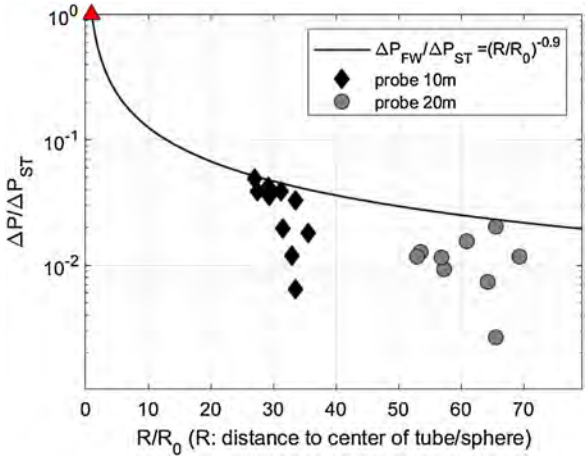

Fig. 27. peak blast overpressure data from (Birk et al., 2007) for 0.4 m^3 tank, propane, various failure pressures and fill levels, failure on top by fire exposure.

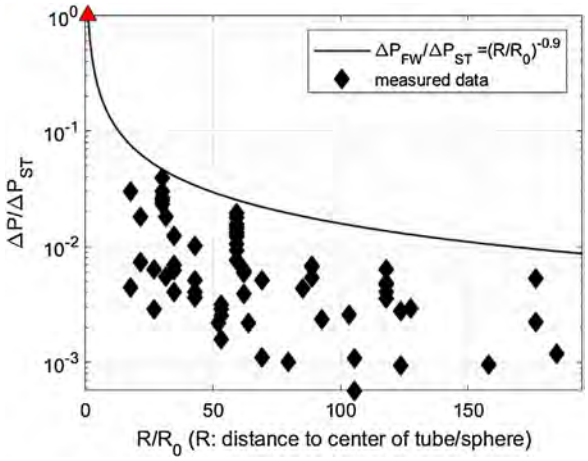

Fig. 28. Peak blast overpressure, British Gas BLEVE tests (Johnson and Pritchard, 1991), various failure pressures and fill levels, 5.7 and 10.8 m^3, Butane and Propane, failure on top by shaped charge.

6.6. Other scales

The method also appears to work very well for the strongest BLEVE blast measured from testing with much larger scales. Fig. 27 includes the tests of (Birk et al., 2007) with 0.4 m^3 propane tanks and Fig. 28 shows the results of the British Gas (BG) tests (Johnson and Pritchard, 1991) with volumes of 5.7 or 11 m^3. Fig. 29 shows the tests of Birk (data presented in (Laboureur et al., 2014)) with volumes of 2 m^3. The BG tests included both propane and butane. For all of these tests the vessel was near the ground and the overpressures were measured at the side or ends – not from the top.

For all these plots, we used the spherical release R_o, not the hemispherical release R_{oh}. Notice that this data is for the far-field (R/Ro > 10) for the tank sides and ends. In the near field, we know there are directional affects where the side and end pressures are lower than the top pressure for top failures. The FW method is for a spherical shock. Here the FW method works very well for the far field. This suggests the directional effects have dissipated and the shock is spherical in the far field.

The model overpredicts the series of data from 2 m^3 tests (Fig. 29). These tests were conducted with smaller heated length on top of the vessel, because the purpose of the investigation was to measure the transition from non-BLEVE failure to BLEVE. Thus this probably led to weaker BLEVE, comparable to short cur length

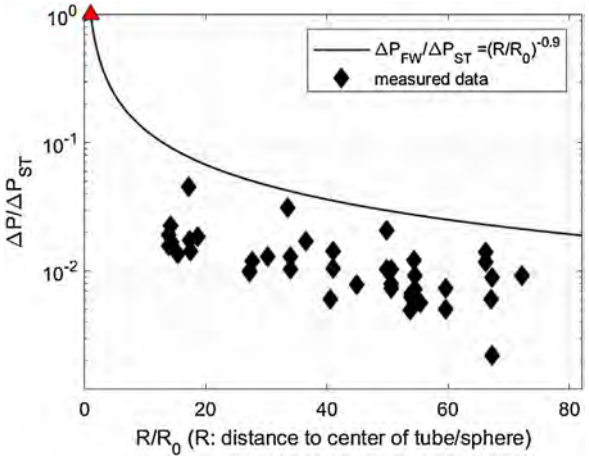

Fig. 29. peak blast overpressure data from Birk experiments (Laboureur et al., 2014) for 2 m^3 tank, propane, various fill levels, failure on top by fire exposure.

BLEVE seen with the small scale apparatus. The prediction is conservative but not exact in this case.

7. Simple method

The data presented in this paper suggests that the prediction of the near-field peak blast overpressure from a BLEVE can be determined using the following equation.

$$\frac{\Delta P_s}{\Delta P_{st}} = \left[\frac{R}{R_o}\right]^{-0.9} \tag{14}$$

where

ΔP_s – is the peak overpressure at the top of the vessel (for top opening vessels) at a distance R from the cylinder centre

ΔP_{st} – is the shock start overpressure from the vapour space using k = 1 for the propane vapour and k = 1.4 for air in the 1D shock tube equation.

R_o – is the radius of a sphere with the same volume as the vapour space when the vessel fails fully

This equation is a fit to the theory for a 1D shock tube, and the Friedman-Whitham theory for spherical shock.

This equation gives the maximum likely overpressure for a rapid opening of the vessel. It does not account for the weakened length. The data suggests a shorter weakened length results in a weaker and faster decaying shock. It also does not account for any local structures that could make the overpressure more directional. In the near-field this overpressure applies to the tank top for top opening. In the far-field it appears to apply to all directions (top, side, end).

The equation is for the strongest possible shock from a given BLEVE with a specific failure pressure, vapour temperature and vapour space volume. Most BLEVEs will produce shocks weaker than this because of the way the vessel opens.

The reader is reminded that the liquid also produces large hazards including ground loading, local drag loading by the flashing liquid, and projectiles. If the release is flammable or toxic then these are also hazards.

8. Conclusions

Small scale BLEVE experiments have been conducted and have produced detailed blast data and high speed images in the near field. Previous literature on this experiment states that lead shock

appears to be caused by the expansion of the vapour space only (Birk et al., 2018). The liquid flashing process is too slow to contribute to this lead shock, and takes place after the lead shock has gone. (Baker et al., 1983) suggested this many years ago.

For the burst pressures considered here the liquid phase change process is too slow to take part in the production of the lead shock. The liquid does produce an overpressure and blast wind that could cause significant damage. This overpressure is not a supersonic shock wave and it dissipates in the near field.

We are not suggesting that the liquid does not produce hazards. Of course the liquid energy dominates the ground force, nearby drag loading of structures from the expanding and flashing liquid and projectile effects.

The relatively slow opening of the vessel results in the lead shock forming at some distance from the wall. For our tests this distance was around 5 times the tube diameter from the tube centre. The overpressure at that position can be determined from the 1D shock tube equation with the decay of the shock strength determined from the Friedman-Whitham method for spherical shocks. Beyond the radius where the shock starts it appears that most BLEVEs will have overpressures lower than the ideal spherical shock calculation. This is probably due to the fact it is not really a perfect spherical release.

The worst case overpressure (from the tank top for top opening vessels) from the vapour space vs distance can be estimated from the burst pressure and temperature and the vapour space volume. This method seems to work well for these small tubes. However preliminary analysis suggests it also works for much larger scales with vessel radius orders of magnitude larger.

This analysis is a physics based model and it is not a curve fit. No energy calculation is required to do this calculation and no adjustment factors are needed to account for other losses.

Other hazards such as ground loading, near-field drag loading from the flashing liquid, and projectiles are dominated by the liquid energy. We are currently working on this data and plan to publish soon.

Declaration of Competing Interest

The authors declare that they have no known competing financial interests or personal relationships that could have appeared to influence the work reported in this paper.

Acknowledgments

This work was a collaboration between the Mechanical and Material Engineering of Queen's University in Canada and the LGEI at IMT Mines Alès in France. It was possible thanks to the funding from the Natural Sciences and Engineering Research Council of Canada with a discovery grant and the effort of the technical team in Alès.

References

Abbasi, T., Abbasi, S.A., 2007. J. Hazard. Mater. 141, 489–519.
Baker, W.E., Cox, P.A., Westine, P.S., Kulesz, J.J., Strehlow, R.A., 1983. Explosion Hazards and Evaluation. Elsevier Scientific Pub. Co.
Baum, M.R., Butterfield, J.M., 1979. J. Mech. Eng. Sci. 21, 253–261.
Baum, M.R., Parry, A.A., 1992. Proc. Inst. Mech. Eng. Part C J. Mech. Eng. Sci. 206, 15–24.
Van den Berg, A.C.C., 2008. Am. Inst. Chem. Eng. Process Saf. Prog. 27, 219–224.
Birk, A.M., Davison, C., Cunningham, M., 2007. J. Loss Prev. Process Ind. 20, 194–206.
Birk, A.M., Heymes, F., Eyssette, R., Lauret, P., Aprin, L., Slangen, P., 2018. Process Saf. Environ. Prot., 116.
Birk, A.M., VanderSteen, J.D.J., 2006. Trans. ASME 128, 648–655.
Casal, J., Salla, J.M., 2006. J. Hazard. Mater. 137, 1321–1327.
Eyssette, R., 2018. Characterization and Modeling of Near-field BLEVE Overpressure and Ground Loading Hazards. Queen's University(Canada), IMT Mines Ales (France).
Johnson, D.M., Pritchard, M.J., 1991. A Large Scale Experimental Study of BLEVEs. British Gas Report No I536, United Kingdom.
Kornegay, W.M., 1965. Production and Propagation of Spherical Shock Waves at Low Ambient Pressures, Distribution.
Laboureur, D., Birk, A.M., Buchlin, J.M., Rambaud, P., Aprin, L., Heymes, F., Osmont, A., 2015. Process Saf. Environ. Prot. 95, 159–171.
Laboureur, D., Heymes, F., Lapebie, E., Buchlin, J.M., Rambaud, P., 2014. Process Saf. Prog. 33, 274–284.
Makino, H., Takeuchi, I., Higuchi, R., 2009. 39–48.
Rothkopf, E.M., Low, W., 1976. Phys. Fluids 19, 1885.
White, F.M., 2008. Fluid Mechanics. McGraw-Hill.
Yakush, S.E., 2016. Int. J. Heat Mass Transf. 103, 173–185.